# SUPPORTING INFORMATION:

## Synergistically enhanced electrical transports properties of $SrTiO_3$ via Fermi level regulating and modulation doping

Dongmei Li[1] ，Dongyang Wang[1], Xiao Zhang[*,1], Li-Dong Zhao[*,1]

[1]*School of Materials Science and Engineering, Beihang University, Beijing 100191, China*

E-mail: zhang_xiao@buaa.edu.cn; zhaolidong@buaa.edu.cn

# EXPERIMENTAL

## Raw materials

Strontium carbonate powders ($SrCO_3$, 99.99%); Titanium dioxide powders ($TiO_2$, 99%); Lanthanum oxide powders ($La_2O_3$, 99.99%); Niobium oxide powders ($Nb_2O_5$, 99.99%) and Titanium boride powders ($TiB_2$, 99.99%).

All samples of this experiment were purchased from Innochem's website and used as received.

## Synthesis

We synthesized $SrTi_{1-x}Nb_xO_3$ ($STN_xO$) (x = 0.1, 0.125, 0.15, 0.175) and $Sr_{1-x}La_xTi_{0.85}Nb_{0.15}O_3$ ($SL_xTNO$) (x = 0.1, 0.125, 0.15) power by solid state reaction (SSR). Raw materials ($SrCO_3$, $TiO_2$, $La_2O_3$ and $Nb_2O_5$) were weighed according to the stoichiometric ratio and ball-milled for 10 h at the speed of 280 rpm. After mixing, the powder is granulated by a tablet press, then placed in a muffle furnace, slowly heated to 1373 K after 5 h, then soaked at this temperature for 6 h, finally cooled to room temperature with the furnace.

The precursor was sintered by spark plasma sintering (SPS) (SPS-211LX, Fuji Electronic Industrial Co., Ltd.) to obtain dense samples. Sintering process as follows: under the pressure of 50 MPa, from 30 K heated to 1273 K for 20 min, and then kept for 5 min. Finally, Φ 12.7 mm × 7.0 mm cylinder sample was obtained.

## Composites

High-purity $TiB_2$ powder (99.999%) and precursor were weighed according to the nominal compositions of $S_{0.875}L_{0.125}T_{0.85}N_{0.15}O_3$ + x% $TiB_2$ (x=0, 2, 3, 4, 5), and then densified by spark plasma sintering (SPS) method (SPS-211LX, Fuji Electronic Industrial Co., Ltd.), the sintering procedure remains unchanged.

## Characterization and testing

**Characterization:** The phase of the powder samples was analyzed by Cu Ka (L = 1.5418 Å) X-ray diffractometer (D/max 2200 PC). The lattice constants of XRD results were calculated by PowDll Converter and Maud software.

**Elastic properties:** The longitudinal ($v_l$) and shear ($v_s$) sound velocities were measured using an ultrasonic instrument (Ultrasonic Pulser/Receiver Model 5058 PR, Olympus, USA). Average sound velocity ($v_a$), Young's modulus ($E$), shear modulus ($G$), Poisson ratio ($v_p$), were calculated from the sound velocities as follows[1]:

$$v_a = \left[\frac{1}{3}\left(\frac{1}{v_l^3} + \frac{2}{v_s^3}\right)\right]^{-1/3} \tag{S1}$$

$$E = \frac{\rho v_s^2 \left(3v_l^2 - 4v_s^2\right)}{\left(v_l^2 - v_s^2\right)} \tag{S2}$$

$$\upsilon_p = \frac{1 - 2\left(v_s / v_l\right)^2}{2 - 2\left(v_s / v_l\right)^2} \tag{S3}$$

$$G = \frac{E}{2\left(1 + \upsilon_p\right)} \tag{S4}$$

$$B = \frac{E}{3 \times (1 - 2\upsilon_P)} \tag{S5}$$

$$\theta_D = \frac{h}{k_B}\left[\frac{3N}{4\pi V}\right]^{1/3} V_a \tag{S6}$$

Where $h$ is Planck's constant, $k_B$ is the Boltzmann constant, $N$ is the number of atoms in a unit cell, $V$ is the unit-cell volume.

**First-principles calculations:** The first-principles calculation in this work was conducted within projector augmented-wave method as implemented in Vienna Ab-initio Simulation Package (VASP)[2, 3]. The Perdew-Burke-Ernzerhof (PBE) functional of the generalized gradient approximation (GGA)[4] was adopted to describe the exchange-correlation. The electronic wave function was expanded in plane waves with cutoff energy 500 eV. A 2 × 2 × 2 supercell ($Sr_8Ti_8O_{24}$) was constructed to describe the one Nb substitution of Ti atom and one La substitution of Sr atom. The inner coordination of atoms was fully relaxed until the residual forces less than 0.01 eV $A^{-1}$ and the total energy converged to $10^{-7}$ eV. The electronic band structures were calculated based on the fully relaxed structures.

**Bandwidth test:** According to equation $\alpha = (1 - R)^2 / 2R$ estimated band gap, where $R$ is reflectivity, $\alpha$ is absorption coefficient and $S$ is scattering coefficient[5].

The reflectivity ($R$) was measured by UV-3600 Plus, in which $BaSO_4$ was used as the reference standard for 100% reflectance.

**Electrical transport properties:** According to $n_H = 1/\left(e \cdot R_H\right)$ and $\mu_H = \sigma \cdot R_H$ measuring carrier concentration and carrier mobility, which $n_H$ is the carrier concentration obtained by Lake Shore 8400, $\mu_H$ is the carrier mobility, and $e$ is the amount of charge[6]. The SPS sintered samples were cut and polished into 3 mm × 3 mm × 10 mm used for Cryoall CTA / ZEM to measure the Seebeck coefficient and conductivity.

**Weighted Mobility:** A simple method to calculate the weighted mobility from Seebeck coefficient and electrical resistivity measurements is introduced. Firstly, we calculated the critical thermoelectric parameter, weighted mobility $\mu_W$, with using the measured data of electrical conductivity and Seebeck coefficient[7, 8]. Based on the SPB model and assuming that the phonon scattering is dominated by acoustic phonons, $m_W$ can be obtained as follows[9, 10]:

$$\mu_w = \frac{3\sigma}{8\pi e F_0(\eta)} \left( \frac{h^2}{2m_e k_B T} \right)^{3/2} \tag{S7}$$

in which e and $m_e$ represent the electron charge and unit mass of free electron, respectively. And $F_n(\eta)$ is the Fermi integral with $n = 0$ and is defined as:

$$F_n(\eta) = \int_0^\infty \frac{x^n}{1+e^{x-\eta}} dx \tag{S8}$$

$$S = \pm \frac{k_B}{e} \left\{ \frac{(r+5/2)\,F_{r+3/2}(\eta)}{(r+3/2)\,F_{r+1/2}(\eta)} - \eta \right\} \tag{S9}$$

where $r$ denotes the scattering factor and equals -1/2 here and $h$ is the reduced chemical potential.

**Calculation for the Lorenz number:** An estimation of $L$ can be made using a single parabolic band (SPB) model with acoustic phonon scattering[11], resulting in a $L$ with a deviation of less than 10% as compared with a more rigorous single non-parabolic band and multiple bands model calculation. Based on the SPB model, the Lorenz number can be given by formula[12]:

$$L=\left(\frac{k_B}{e}\right)^2\left(\frac{(r+7/2)F_{r+5/2}(\eta)}{(r+3/2)F_{r+1/2}(\eta)}-\left[\frac{(r+5/2)F_{r+5/2}(\eta)}{(r+3/2)F_{r+1/2}(\eta)}\right]^2\right) \tag{S10}$$

where $k_B$ is the Boltzmann constant, $e$ is the electric charge, $r$ is the scattering rate, and $\eta$ refers to the reduced Fermi energy, which can be derived from the measured Seebeck coefficients with consideration of acoustic phonon dominated scattering ($r$ = -1/2) via the following equation:

$$S=\frac{k_B}{e}\left[\frac{(r+5/2)F_{r+3/2}(\eta)}{(r+3/2)F_{r+1/2}(\eta)}-\eta\right] \tag{S11}$$

$$F_x(\eta)=\int_0^\infty\frac{\varepsilon^x}{1+\exp(\varepsilon-\eta)}d\varepsilon \tag{S12}$$

$$\eta=\frac{E_f}{k_B T} \tag{S13}$$

where $F_x(\eta)$ is Fermi integral and $E_f$ is the Fermi energy.

**Quality factor B:** The material quality factor $B$, is designed to estimate the optimal thermoelectric performance for specified materials by the effective mass model . $B$ is initially defined as[13]:

$$B=9\frac{\mu_W}{\kappa_{lat}}\left(\frac{T}{300}\right)^{5/2} \tag{S14}$$

where $\mu_W$ is Weighted mobility and $\kappa_{lat}$ is the lattice thermal conductivity.

**Thermal transport properties:** Prepared the sample of 6 mm × 6 mm×(~1.2 mm) by cutting, grinding and spraying. Then according to the formula $\kappa_{tot}=D\rho C_P$ [14] got the thermal conductivity, where the thermal diffusion coefficient D is obtained through the test of laser thermal conductivity instrument equipment (LFA-457), and the sample density $\rho$ is obtained by the sample mass to volume ratio[14]. The electronic thermal conductivity ($\kappa_{ele}$) was calculated by $\kappa_{ele}=L\sigma T$, where the Lorenz number was calculated based on a single parabolic band (SPB) model. Then the lattice thermal conductivity ($\kappa_{lat}$) could be obtained via the relationship: $\kappa_{lat}=\kappa_{tot}-\kappa_{ele}$ The uncertainty of the thermal conductivity is estimated to be within 8%, and the combined uncertainty for all measurements involved in the calculation of $ZT$ is within 20%.

**Table S1** Calculated anisotropic effective mass of triple-fold CBM.

| $m^*$ ($m_e$) | *Γ-R* | *Γ-X* | *Γ-M* |
|---|---|---|---|
| 1 | 0.73 | 6.58 | 0.90 |
| 2 | 0.58 | 0.40 | 0.67 |
| 3 | 0.58 | 0.40 | 0.43 |

**Table S2** Physical constants for experimental and theoretical calculation of $SrTiO_3$

| Physical constants | Experimental | Theoretical caculation |
|---|---|---|
| Longitudinal sound velocity, $v_l$ (m $s^{-1}$) | 8027 | 8252 |
| Shear sound velocity, $v_s$ (m $s^{-1}$) | 4816 | 4847 |
| Average sound velocity, $v_a$ (m $s^{-1}$) | 5230 | 5373 |
| Young's modulus, $E$ (GPa) | 234 | 289 |
| Shear modulus, $G$ (GPa) | 115 | 117 |
| Bulk modulus, $B$ (GPa) | 166 | 183 |
| Debye temperature, $\Theta_d$ (K) | 682 | 694 |

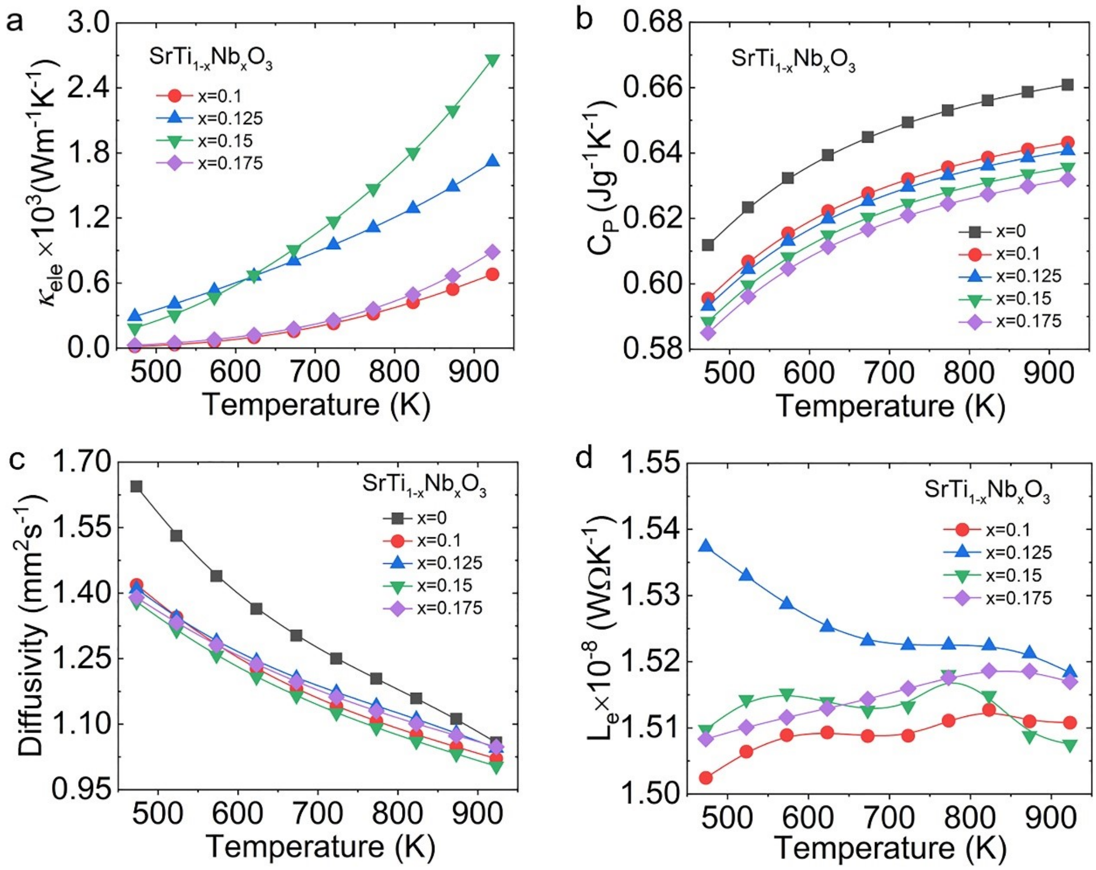


**Fig. S1** Temperature dependence of (a) electronic thermal conductivity; (b) specific heat; (c) thermal diffusivity and (d) Lorenz number of $SrTi_{1-x}Nb_xO_3$ (x = 0-0.175)

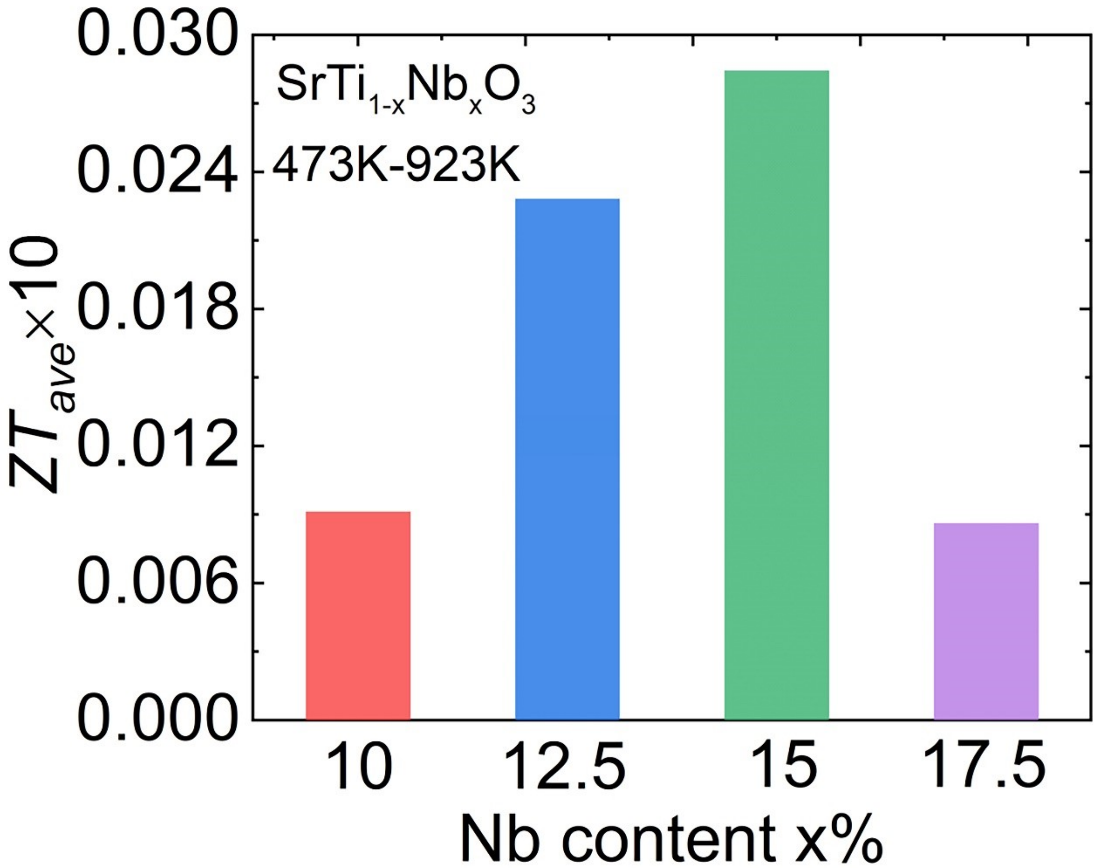


**Fig. S2** Average *ZT* ($ZT_{ave}$) between 473 and 923 K of $SrTi_{1-x}Nb_xO_3$ (x = 0.1-0.175)

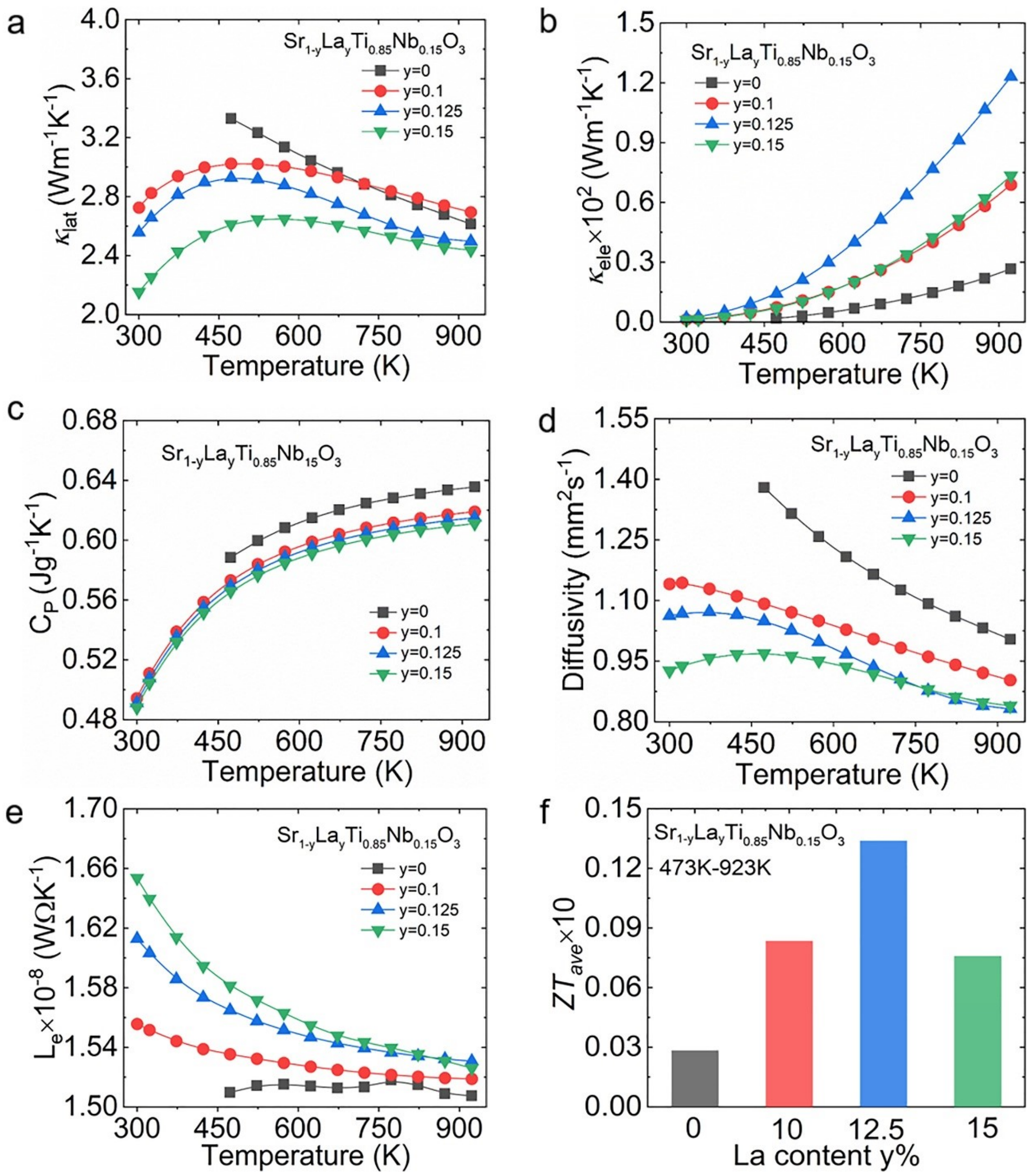


**Fig. S3** Temperature dependence of (a) lattice thermal conductivity; (b) electronic thermal conductivity; (c) specific heat; (d) thermal diffusivity and (e) Lorenz number; (f) average *ZT* ($ZT_{ave}$) between 473 and 923 K of $Sr_{1-y}La_yTi_{0.85}Nb_{0.15}O_3$ (y = 0-0.15)

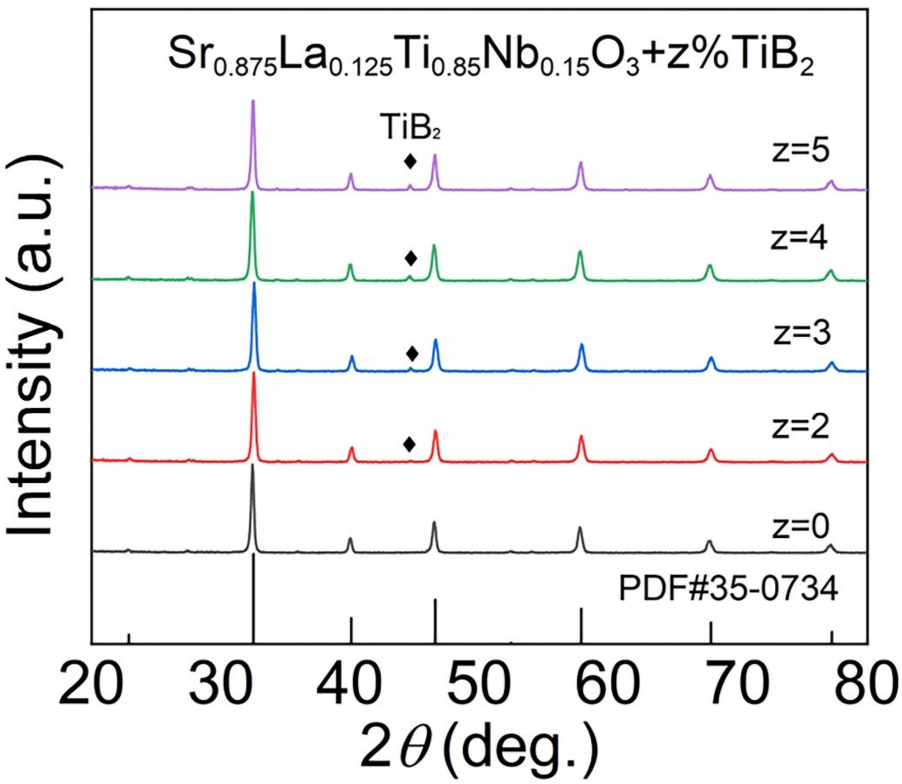


**Fig. S4** Powder XRD pattern of $Sr_{0.875}La_{0.125}Ti_{0.85}Nb_{0.15}O_3$ + z% $TiB_2$

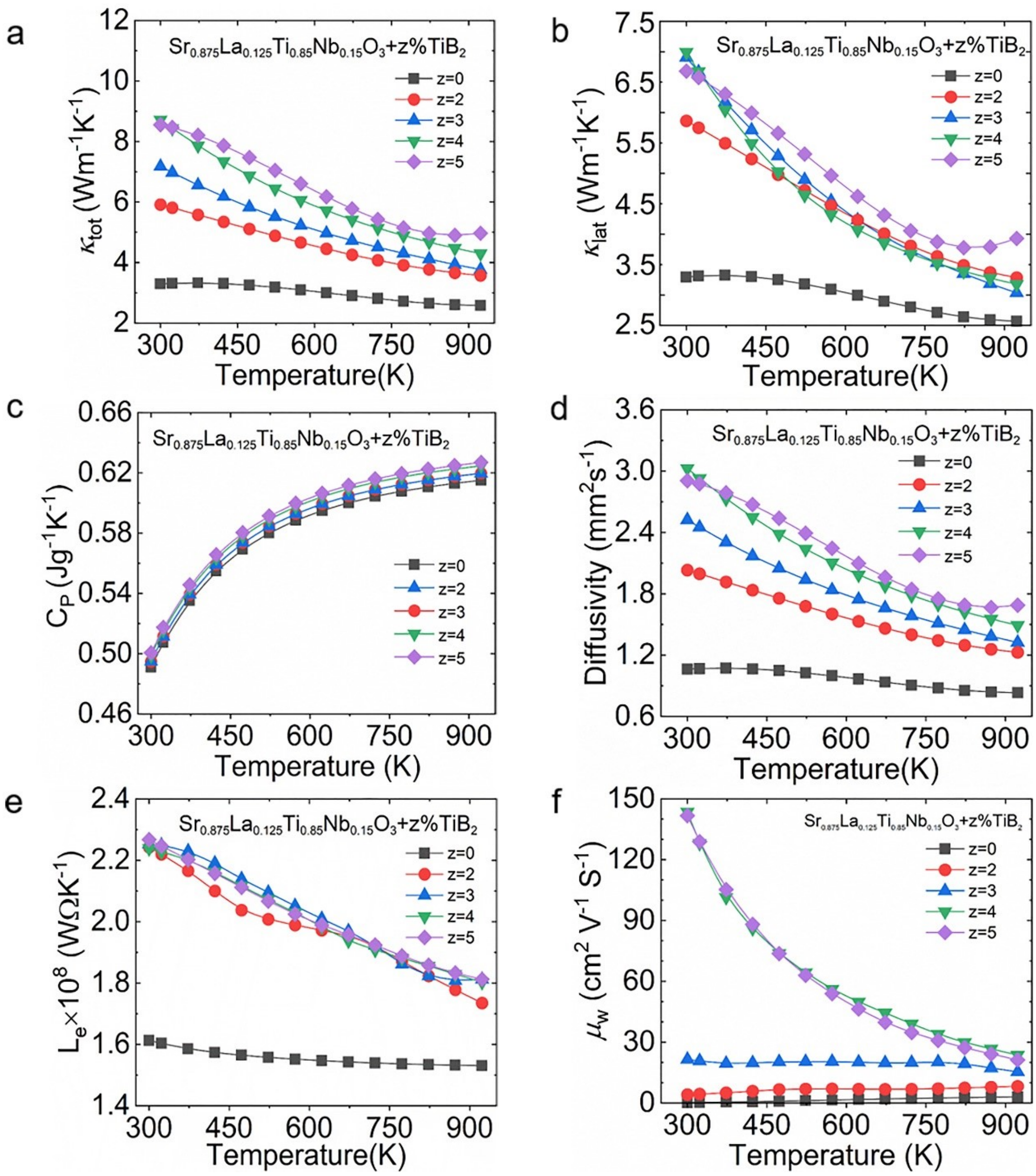


**Fig. S5** Temperature dependence of (a) total thermal conductivity; (b) lattice thermal conductivity (c) specific heat; and (d) thermal diffusivity; (e) Lorenz number and (f) weighted mobility of $Sr_{0.875}La_{0.125}Ti_{0.85}Nb_{0.15}O_3$ + z% $TiB_2$(x =0-5)

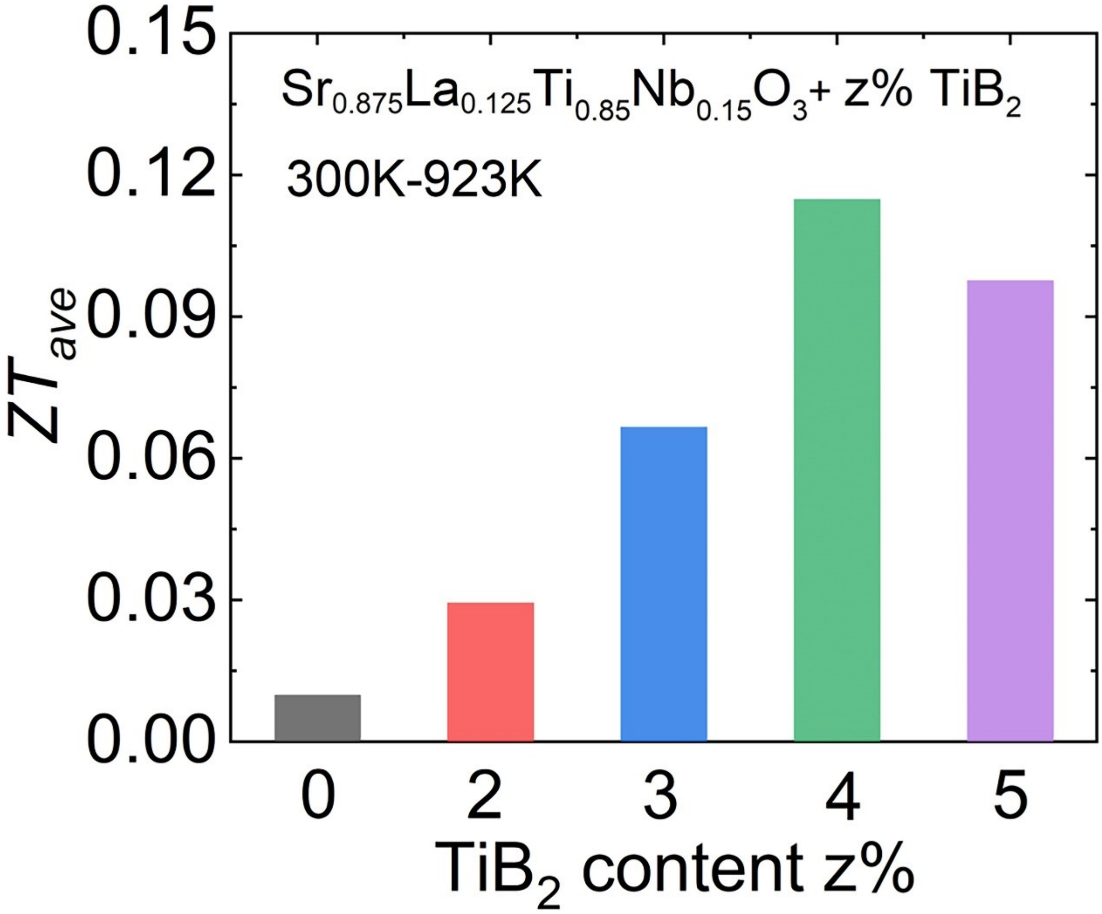


**Fig. S6** Average *ZT* ($ZT_{ave}$) between 300 and 923 K of of $Sr_{0.875}La_{0.125}Ti_{0.85}Nb_{0.15}O_3$ + z% $TiB_2$(x =0-5)

**Table S3** Thermoelectric transport properties at 923 K of all samples.

| Samples | Electrical Conductivity (S cm$^{-1}$) | Seebeck Coefficient (μV K$^{-1}$) | Power Factor (μW cm$^{-1}$ K$^{-2}$) | Thermal Conductivity (W m$^{-1}$ K$^{-1}$) | *ZT* |
|---|---|---|---|---|---|
| $SrTi_{0.9}Nb_{0.1}O_3$ | 0.4887 | -450.06 | 0.0990 | 2.9555 | 0.0031 |
| $SrTi_{0.875}Nb_{0.125}O_3$ | 1.2262 | -360.55 | 0.1594 | 2.6782 | 0.0055 |
| $SrTi_{0.85}Nb_{0.15}O_3$ | 1.9172 | -357.80 | 0.2454 | 2.6167 | 0.0087 |
| $SrTi_{0.825}Nb_{0.125}O_3$ | 0.6335 | -410.89 | 0.1070 | 2.6491 | 0.0037 |
| $Sr_{0.9}La_{0.1}Ti_{0.85}Nb_{0.15}O_3$ | 5.2713 | -373.26 | 0.7344 | 2.7019 | 0.0187 |
| $Sr_{0.875}La_{0.125}Ti_{0.85}Nb_{0.15}O_3$ | 8.7199 | -320.82 | 0.8975 | 2.5096 | 0.0330 |
| $Sr_{0.85}La_{0.15}Ti_{0.85}Nb_{0.15}O_3$ | 5.1994 | -335.98 | 0.5869 | 2.4441 | 0.0222 |
| $Sr_{0.875}La_{0.125}Ti_{0.85}Nb_{0.15}O_3$+2%$TiB_2$ | 178.8307 | -149.76 | 4.0110 | 3.5589 | 0.1040 |
| $Sr_{0.875}La_{0.125}Ti_{0.85}Nb_{0.15}O_3$+3%$TiB_2$ | 438.5366 | -127.88 | 7.1716 | 3.7860 | 0.1748 |
| $Sr_{0.875}La_{0.125}Ti_{0.85}Nb_{0.15}O_3$+4%$TiB_2$ | 668.8567 | -128.44 | 11.0356 | 4.3900 | 0.2320 |
| $Sr_{0.875}La_{0.125}Ti_{0.85}Nb_{0.15}O_3$+5%$TiB_2$ | 616.2383 | -126.23 | 9.8196 | 5.1351 | 0.1765 |

## REFERENCES


1. Yu. Xiao, Cheng. Chang, Yanling. Pei, Di, Wu, Kunling and Peng, *Physical Review B*, 2016, **94**, 125-203.
2. G. G. Kresse and J. J. Furthmüller, *Physical Review. B, Condensed matter*, 1996, **54**, 11169.
3. P. E. Blochl, *Physical Review B*, 1994, **50**, 17953-17979.
4. M. Ernzerhof, *Physical Review Letters*, 1996, **77**, 3865-3868.
5. WK. He, DY. Wang, and Y. Xiao, *Science*. 2019, **365**, 1418-1424.
6. D. Wu, L. D. Zhao, X. Tong, W. Li, L. Wu, Q. Tan, Y. Pei, L. Huang, J. F. Li and Y. Zhu, *Energy & Environmental Science*, 2015, **8**, 2056-2068.
7. J. Mao, J. Shuai, S. Song, Y. Wu and Z. Ren, *Proceedings of the National Academy of Sciences of the United States of America*, 2017, **114**, 10548-10553.
8. Z. Alex, D. M. Smiadak, J. L. Blackburn, A. J. Ferguson, M. L. Chabinyc, D. Olivier, J. Wang, K. Kirill, M. Joshua and L. T. Schelhas, *Applied Physics Reviews*, 2018, **5**, 021303.
9. Xiao, Wang, Dongyang, Zhang, Yang, Chen, Congrun, Zhang, Shuxuan and Wang, *Journal of the American Chemical Society*, 2020, **142(8)**, 4051-4060.
10. Kuo, Jimmy, Jiahong, Kang, Stephen, Dongmin, Imasato, Kazuki, Tamaki and Hiromasa, *Energy & Environmental Science*, 2018, **11**, 429-434.
11. A. F. May, E. S. Toberer, A. Saramat and G. J. Snyder, *Physical Review. B, Condensed matter*, 2009, **80**, 5959150.
12. H. Pang, X. Zhang, D. Wang, R. Huang and L. D. Zhao, *Journal of Materiomics*, 2021, **8**, 184-194.
13. S. D. Kang and G. J. Sny De R, *Nature Materials*, 2017, **16**, 252-257.
14. W. W. Qu, X. X. Zhang, B. F. Yuan, L. D. Zhao, S. Scienceengineering, B. University and C. N. P. C. G. D. Company, *Rare Metals*, 2018, **37**,79-84.